American Mineralogist, Volume 66, pages 410–423, 1981

Natroapophyllite, a new orthorhombic sodium analog of apophyllite
I. Description, occurrence, and nomenclature

HIROHARU MATSUEDA

Institute of Mining Geology
Akita University, Akita 010, Japan

YASUNORI MIURA[1] AND JOHN RUCKLIDGE

Department of Geology, University of Toronto
Toronto, Ontario M5S 1A1, Canada

Abstract

Natroapophyllite $NaCa_4Si_8O_{20}F \cdot 8H_2O$, a sodium analog of apophyllite, has been found in white skarn at the Sampo Mine, Okayama, Japan. Electron microprobe analysis of the mineral gives SiO_2 52.79, CaO 25.41, Na_2O 3.05, K_2O 0.33, F 2.27, H_2O (by difference) 17.11 weight percent; ($-O \equiv F_2 = 0.96$). Optical and crystallographic parameters are: $\alpha = 1.536(2)$, $\beta = 1.538(2)$, $\gamma = 1.544(2)$, 2V(meas.) = 32(1)°, $r < v$; $a = 8.875(4)$, $b = 8.881(6)$, $c = 15.79(1)$Å, space group *Pnnm*, Z = 2; *D* obs. = 2.50, *D* calc. = 2.30 g/cm^3.

The crystal structure, refined ($R = 0.056$) by least-squares methods from 563 diffuse X-ray reflections collected with an automatic single-crystal diffractometer, has rings of SiO_4 tetrahedra. Ca- and Na-polyhedra are more distorted in natroapophyllite compared with apophyllite because of the substitution of Na for K. TGA shows discontinuous water loss of 16 weight percent, similar to apophyllite. DTA and IR data suggest that natroapophyllite has hydrogen atoms in three different structural environments.

A pseudo solid-solution series exists between natroapophyllite and fluorapophyllite which bridges the orthorhombic–tetragonal symmetry change. Crystals are shown which display continuous and discontinuous zoning.

Introduction

The nomenclature of the apophyllite group is complex. Fluorapophyllite and hydroxyapophyllite have recently been defined by Dunn *et al.* (1978) as the valid names for the end members of the tetragonal apophyllite series, in which K is the major alkali cation. Orthorhombic varieties of apophyllite have also been described. Sahama (1965) gave details of an orthorhombic fluorine-rich apophyllite $KCa_3AlSi_8O_{20}F \cdot 8H_2O$, which contained significant Al.

Although Na may substitute for K in apophyllite to a small degree, samples in which Na predominates over K have only recently been described (Matsueda, 1975, 1980; Miura *et al.*, 1976; Miura, 1977; Miura and Rucklidge, 1979). The Na-rich examples are invariably orthorhombic and fluorine-rich, and the name natroapophyllite has been proposed for this sodium analog of the orthorhombic apophyllite described originally by Sahama (1965) and Belsare (1969). It is not the sodium analog of ordinary tetragonal apophyllite. The name natroapophyllite, given in allusion to its compositional relation to apophyllite, was approved by the IMA Commission on New Minerals and New Mineral Names in October, 1976. Other additional prefixes for natroapophyllite would be in order, *e.g.*, ortho- and fluor-, but in the absence of non-orthorhombic or other than fluorine-rich natroapophyllite, it seems unnecessary to burden the literature with more complex names than natroapophyllite, which is defined as being the orthorhombic sodium end member of the apophyllite group minerals with the formula $NaCa_4Si_8O_{20}F \cdot 8H_2O$.

[1] On leave from Department of Mineralogical Sciences and Geology, Faculty of Science, Yamaguchi University, Yamaguchi 753, Japan.

0003–004X/81/0304–0410$02.00

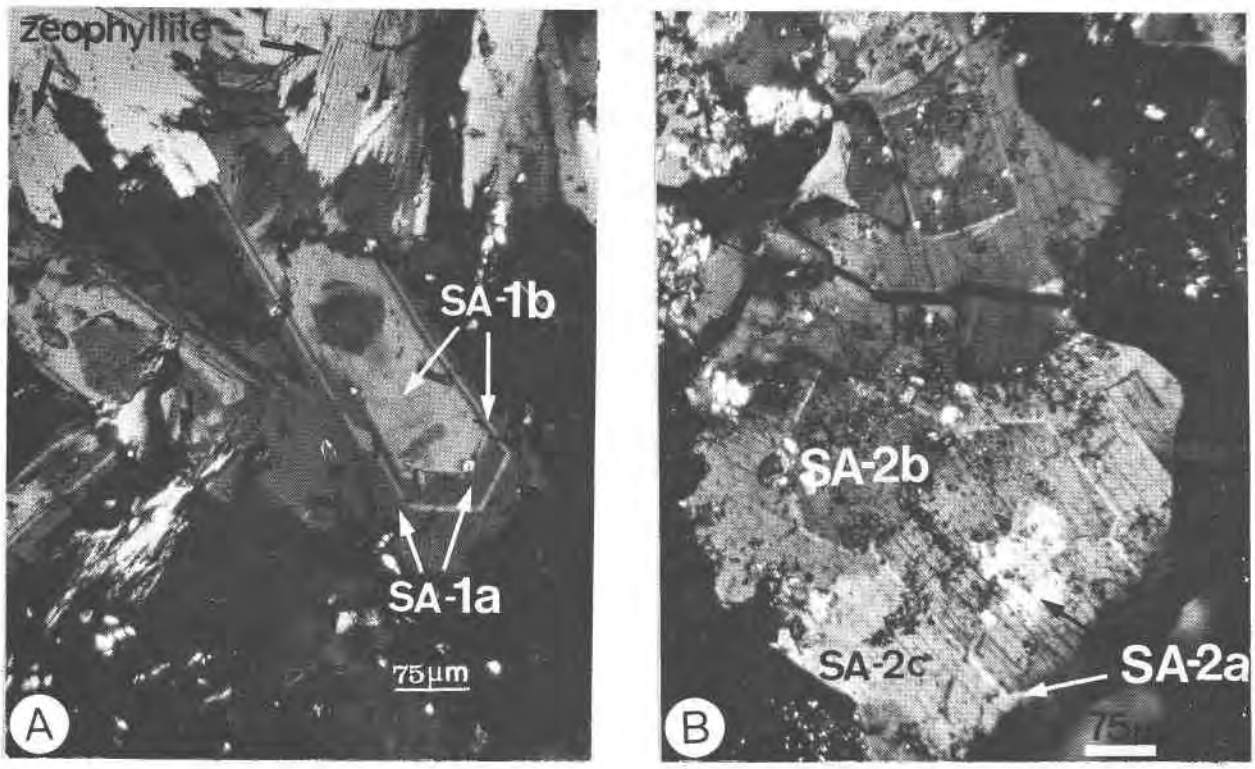

Fig. 1. Optical micrographs of natroapophyllite from the Sampo Mine. (a) Composite crystals of typical natroapophyllite (SA-1b) and fluorapophyllite (SA-1a). SA-1 samples are up to 0.15 × 1 mm. (b) Composite natro– (SA-2a) fluorapophyllite (SA-2b) crystals and intermediate compositions (SA-2c, d, e).

Sample descriptions, physical properties, and morphology

The four samples described here have SA-numbers referring to the Sampo Mine, some 10 km west of Takahashi City in Okayama Prefecture. The Sampo Mine is one of the typical contact metasomatic ore deposits of the Chuhgoku Province and was emplaced at the contact of Paleozoic limestone and slate with Late Cretaceous granite (Matsueda, 1973, 1980). Natroapophyllite occurs in association with zeophyllite, cuspidine, apophyllite, and calcite in the "white skarn" on the 9th level, No. 1 Yoshiki Ore Body of the mine. Other associated minerals include andradite, xonotlite, wollastonite, a clinopyroxene in the diopside–hedenbergite series, magnetite, quartz, and native bismuth, all of which occur in banded zones between the granite and marble contacts. Natroapophyllite was found in the white skarns close to the marble contact (Matsueda, 1973, 1980). The fluorine-bearing silicates zeophyllite and apophyllite crystallized during a hydrothermal alteration stage, which occurred after the thermal metamorphism and skarn generation by the granite intrusion (Matsueda, 1980). The white skarn was formed by fluorine metasomatism of ferrobustamite and wollastonite–andradite skarns (Matsueda, 1980). In transmitted light the grains of natroapophyllite are invariably rimmed by apophyllite (Fig. 1), which suggests that a pseudo solid solution exists between apophyllite and natroapophyllite, in which there is a transition from tetragonal to orthorhombic symmetry. This would represent a range of chemical variation beyond the solid-solution series fluorapophyllite to hydroxyapophyllite reported by Dunn *et al.* (1978) and Dunn and Wilson (1978).

Natroapophyllite samples SA-1 to 3 in Table 1 occur as minute prismatic euhedral to subhedral crystals up to 0.15 × 1 mm (Figs. 1 and 2), brownish-yellow to yellowish-brown (in SA-1 and 3) or colorless to white (in SA-2). The luster is vitreous to pearly. A typical example of natroapophyllite in SA-1 is zoned with fluorapophyllite, and the two phases are referred to in Table 1 as SA-1b and SA-1a, respectively. Composite crystals exhibit {100} prisms truncated by the {111} dipyramid striated perpendicular

Table 1. Occurrences, parageneses, compositions, and optic axial angles of fluorapophyllite and natroapophyllite from the Sampo Mine

Specimen No.	Occurrence	Paragenesis	Alkali content*	2V(meas.)
SA-1a	White skarn (9L No.1 Yoshiki Ore Body)	Zeophyllite, calcite, andradite, fluorite, cuspidine	$K_{1.08}Na_{0.02}Ca_{4.13}$	0°
SA-1b			$K_{0.06}Na_{0.90}Ca_{4.13}$	≃32°
SA-2a	Druse in white skarn (9L No.1 Yoshiki Ore Body)	Magnetite, andradite, fluorite	$K_{0.03}Na_{0.86}Ca_{4.08}$	≃31°
SA-2b			$K_{1.01}Na_{0.02}Ca_{4.09}$	≫ 0°
SA-2c			$K_{0.40}Na_{0.28}Ca_{4.00}$	> 0°
SA-2d			$K_{0.85}Na_{0.10}Ca_{4.16}$	?
SA-2e			$K_{1.09}Na_{0.03}Ca_{4.01}$	?
SA-3a	White skarn (9L West No.1 Yoshiki Ore Body)	Fluorite, xonotolite, andradite, magnetite, cuspidine	$K_{0.07}Na_{0.75}Ca_{4.12}$	≃30°
SA-3b			$K_{0.45}Na_{0.51}Ca_{4.12}$	?
SA-3c			$K_{0.95}Na_{0.03}Ca_{4.20}$	?
SA-4	Spherical skarn in marble (10L West No.1 Yoshiki Ore Body)	Fluorite, andradite	$K_{0.90}Na_{0.03}Ca_{4.13}$	> 0°

* *Atomic ratios of alkali ions on the basis of Si = 8.00.*

to the *c* axis (Fig. 1a). Specimen SA-2 is subdivided 2a–2e for varying compositions in the range natro- to fluorapophyllite. It exhibits well-developed {111} dipyramids with {100} prisms which give the sample a "fish-eye" appearance (Figs. 1b and 2).

The external morphology of the crystals is similar to that of fluorapophyllite (Figs. 1 and 2) because, as shown below, the crystals are composites with the rims being K-rich fluorapophyllite and the cores Na-rich natroapophyllite. Optical measurement could be

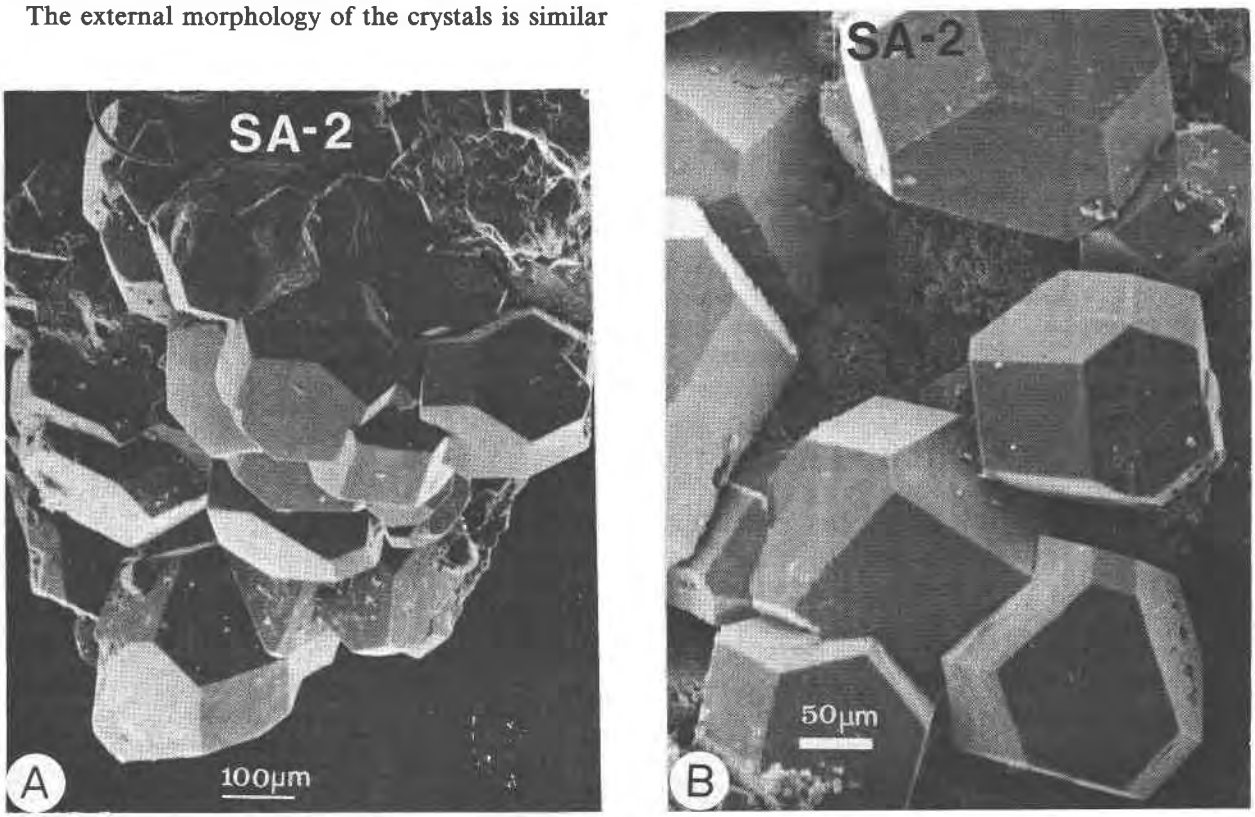

Fig. 2. Scanning electron micrographs of natroapophyllite (SA-2a). (a) Subhedral crystals of SA-2 showing 'fish eye' appearance. (b) Euhedral crytsals of SA-2.

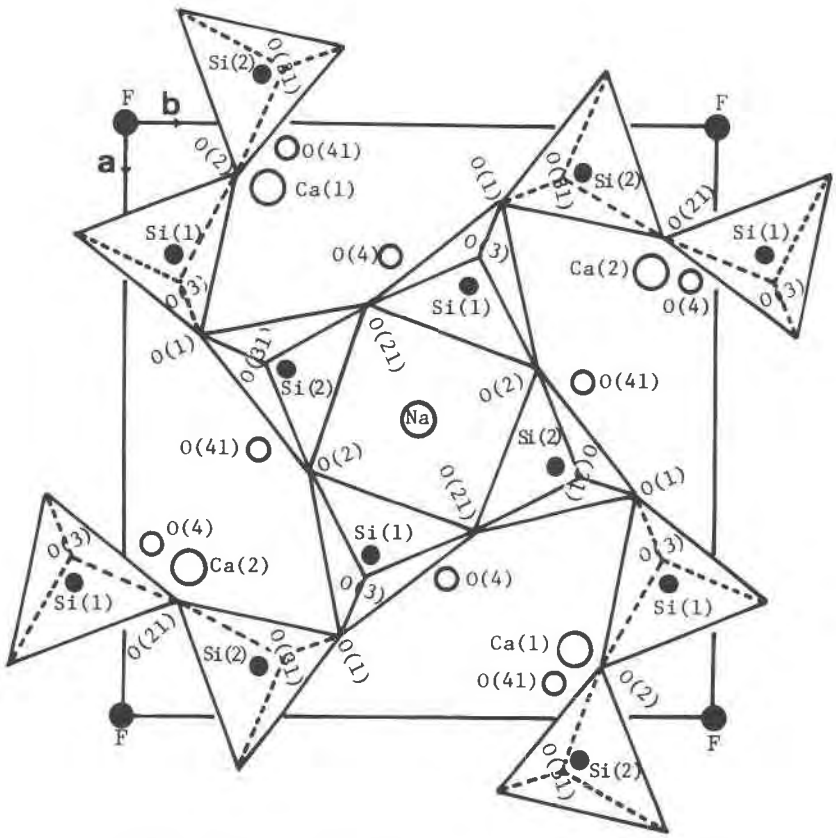

Fig. 3. The Si_8O_{20} sheet in natroapophyllite projected on (001).

made most reliably on specimen SA-1 in which the K and Na phases are easily distinguished. The Na-rich component is colorless in thin section and distinctly biaxial with 2V(meas.) = 32(1)°, $r < v$; $\alpha = 1.536(2)$, $\beta = 1.538(2)$ and $\gamma = 1.544(2)$. The K-rich component is uniaxial with the properties of normal fluorapophyllite, $\omega = 1.536$ and $\epsilon = 1.539$ (see Table 1). Biaxial examples of the K-rich component are also noted in Table 1, but the detailed description of these phases will be reserved for a separate paper.

Cleavage is perfect on {001} and poor on {110}. The Mohs hardness is 4 to 5, and the streak is light gray. The mineral does not fluoresce in UV radiation. An IR spectrum of natroapophyllite is shown in Part II. The powder used for this was carefully separated from the K-rich fluorapophyllite parts of the crystals. The spectrum shows two sharp peaks at 3560 and 3420 cm^{-1} and one broad peak at 3020 cm^{-1}. These correspond to two strong and one weak hydrogen bonds (see Part II). The specific gravity, measured by the suspension method in Thoulet's solution on somewhat impure materials including small amounts of calcite and fluorite is 2.50, and the calculated value is 2.30. Natroapophyllite is slightly soluble in 1:1 HCl and 1:1 HNO_3.

Chemistry

The chemical compositions of the natroapophyllite and fluorapophyllite crystals were determined with the JXA-5A electron microprobe analyzer at Kyūshū University. The analyses, which were performed at 15kV accelerating voltage and 15nA sample current, are shown in Table 2, along with a list of the standards used. Water was determined by difference. No other elements besides those listed were detected in either form of apophyllite from the Sampo Mine. Wet-chemical analysis of somewhat impure material including a small amount of apophyllite from the same locality was performed by Dr. K. Ishibashi of Fukuoka University, using weight loss on ignition. The results are $H_2O(+) = 15.83$ and $H_2O(-) = 0.14$ weight percent. An analysis of the most Na-rich specimen (SA-1b) with 3.05 weight percent Na_2O is presented in Table 2. We define this as the type compo-

Table 2. Microprobe analyses of fluorapophyllite and natroapophyllite

	SA-1b Natroapophyllite (Wt.%)*	(Atomic Ratio)**		SA-2a Natroapophyllite (Wt.%)*	(Atomic Ratio)**		SA-1a (Wt.%)*	SA-2b (Wt.%)*	SA-2c (Wt.%)*	SA-2e (Wt.%)*	SA-3a (Wt.%)*	SA-3b (Wt.%)*	SA-3c (Wt.%)*	SA-4 (Wt.%)*
SiO_2	52.79	Si	8.00	53.46	Si	8.00	51.61	51.26	52.67	52.11	51.85	52.08	52.09	51.66
Al_2O_3	0.00	Al	0.00	0.00	Al	0.00	0.00	0.01	0.00	0.00	0.00	0.00	0.00	0.00
Fe_2O_3	-----	Fe	----	0.02	Fe	0.002	-----	0.01	0.00	0.01	0.05	0.02	0.01	0.03
CaO	25.41	Ca	4.13	25.43	Ca	4.08	24.84	24.49	24.61	24.39	24.90	25.06	25.54	24.90
MgO	-----	Mg	----	0.00	Mg	0.00	-----	0.02	0.04	0.01	-----	-----	-----	-----
MnO	-----	Mn	----	0.00	Mn	0.00	-----	0.00	0.04	0.05	-----	-----	-----	-----
Na_2O	3.05	Na	0.90	2.95	Na	0.86	0.08	0.20	0.96	0.11	2.50	1.71	0.26	0.09
K_2O	0.33	K	0.06	0.18	K	0.03	5.47	5.06	2.08	5.58	0.38	2.29	4.84	4.56
F	2.27	F	1.09	2.25	F	1.06	2.32	2.61	2.54	2.40	2.72	2.64	2.83	2.51
$H_2O(+)$	(17.11)	O	29.88	(16.66)	O	28.67	(16.66)	(17.44)	(18.13)	(16.35)	(18.75)	(17.31)	(15.62)	(17.31)
Total	100.96			100.95			100.98	101.10	101.07	101.01	101.15	101.11	101.19	101.06
$O \equiv F_2$	0.96			0.95			0.98	1.10	1.07	1.01	1.15	1.11	1.19	1.06
	(100.00)			(100.00)			(100.00)	(100.00)	(100.00)	(100.00)	(100.00)	(100.00)	(100.00)	(100.00)

** On the basis of Si = 8.00.*

*** Standards used in the electron microprobe analyses are synthetic $CaSiO_3$(for Ca and Si); Al_2O_3(Al); MgO(Mg); analyzed hematite(Fe); manganosite(Mn); albite from Amelia(Na); orthoclase(K); and fluorite(F).*

sition for natroapophyllite, for which the formula is:

$$(Na_{0.90}K_{0.06})_{0.96}Ca_{4.13}Si_{8.00}F_{1.09}O_{20.07} \cdot 8.6H_2O$$

on the basis of Si = 8.00. Type material of natroapophyllite SA-3, which resembles the SA-1 specimen, is deposited in the National Science Museum, Shinjuku, Tokyo and Institute of Mining Geology, Mining College, Akita University, Akita.

The composition of uniaxial (or biaxial, see Table 1) K-rich apophyllite, which usually rims the natroapophyllite, was also determined by electron microprobe analysis and is shown in Table 2.

Chemical zoning can be seen in the microprobe analyses of Table 2. In the case of SA-1 only the Na and K extremes are seen, and the zoning is discontinuous, sometimes oscillating. Specimens SA-2 and SA-3 show intermediate compositions as well, and from this evidence we propose the existence of a solid-solution series. However, there are optical discontinuities in these two samples, with the light regions being Na-rich and the dark K-rich (see Fig. 1b). It is difficult to establish the precise optical properties of the parts of the crystals with intermediate compositions. Therefore it is not clear at what composition the orthorhombic–tetragonal transition occurs or whether gaps exist in the solid-solution series. Some of the zoning has the appearance of compositional change taking place during growth (SA-1), while in SA-2 the zoning appears more characteristic of alteration. However, in general the outer zone is K-rich fluorapophyllite, and the inner regions are Na-rich natroapophyllite.

The analysis of the intermediate zone in SA-2 is deficient in alkalis, and the missing cations may be Li^+ or H_3O^+, neither of which can be measured by electron probe microanalysis.

These data support the proposition that natroapophyllite is chemically an orthorhombic sodium equivalent of fluorapophyllite.

X-ray crystallography

The unit-cell dimensions refined from 15 reflections collected with a Syntex $P\bar{1}$ automated single-crystal diffractometer, from a single crystal of natroapophyllite (SA-1), are $a = 8.875(4)$, $b = 8.881(6)$, $c = 15.79(1)$Å; $V = 1236.9$Å^3 and $Z = 2$. The space group was assigned as *Pnnm* or *Pnn*2 on the basis of Weissenberg film data. The unit-cell dimensions of the SA-1a specimen are distinctly larger than those of typical natroapophyllite (SA-1b) because of the partial K substitution for Na.

X-ray powder diffractometer data for natroapophyllite SA-1b are given in Table 3, where the values of *d*calc. and *hkl* were obtained from the computer program of Appleman and Evans (1973). Spurious lines attributed to minor amounts of fluorite and zeophyllite have been omitted. The remaining lines, which do not show clearly the splitting which would be required by orthorhombic symmetry, are presented as single values, thus making the pattern in-

Table 3. X-ray powder diffraction data for natroapophyllite (SA-1b); fluorapophyllite (SA-1a) impurities may have been included in the sample material

d_{calc}* (Å)	*hkl**	d_{obs}** (Å)	I_{obs}	d_{calc}* (Å)	*hkl**	d_{obs}** (Å)	I_{obs}
7.89	002	7.83	20	2.645	132	2.68	1
7.74	101,011	7.77	18	2.642	312		
6.28	110	6.28	4	2.476	133	2.50	18
4.525	013,103	4.54	19	2.473	313		
4.436	020,200	4.45	10	2.470	125	2.48	24
3.974	004	3.96	100	2.466	215		
3.861	202	3.88	14	2.425	116	2.44	9
3.850	211,121	3.87	14	2.350	322	2.38	2
3.546	122	3.57	17	2.229	323	2.25	1
3.543	212			2.184	107	2.19	5
3.337	114	3.36	17	2.154	305,140	2.17	2
3.141	220	3.15	16	2.153	410		
2.975	015	2.98	63	2.134	141	2.15	2
2.970	105			2.132	411		
2.916	222	2.93	9	2.097	135	2.11	10
2.909	031			2.094	315		
		2.92	9				
2.907	301			2.087	234,324	2.10	5
2.810	130	2.83	3	2.022	332	2.03	2
2.806	310			1.987	420,240	2.00	5
2.797	124						
		2.82	5				
2.795	214						
2.764	131	2.80	2				
2.762	311						

* *Indices and d_{calc} were obtained using the computer program of Appleman and Evans (1973).*

** *X-ray diffractometer conditions are : Cu/Ni radiation, $CuK\alpha_1$= 1.54050Å; Si used as internal standard; scanned at ¼ 2θ per minute.*

distinguishable from a tetragonal one. However, the shapes of peaks on the powder diffractogram are broadened and distorted in such a way as to suggest that they are composite. The powder diffractometer does not have high enough resolution to provide the separation necessary, and unfortunately it was not possible to use Guinier methods. Based on the single crystal and optical data, there is no doubt that material is in fact orthorhombic. The consistent slight excess of *d*obs. over *d*calc. suggests that some of the K-rich fluorapophyllite has been included in the powder along with natroapophyllite.

Discussion

Analogous to the alkali feldspars, where the degree of substitution of Na and K varies with temperature and composition, fluorapophyllite and natroapophyllite may demonstrate the same restricted Na–K exchange. A further analogy can be drawn between apophyllite and the alkali feldspars in that in each group K-rich phases have higher symmetry than Na-rich phases. In the following scheme fluorapophyllite (tetragonal) and sanidine/orthoclase (monoclinic) are analogous to natroapophyllite (orthorhombic) and high albite (triclinic). The analogy goes further when one considers that lower symmetry versions of the K-rich phases also occur, *viz.* orthorhombic K-apophyllite and triclinic microcline. The reasons for these symmetry similarities undoubtedly lie in the way the tetrahedral framework becomes puckered by the substitution of the smaller Na ion for K in both groups (Ribbe, 1975). The diadochy between F and OH is structurally convenient because of their similar ionic radii and unit charges, hence the existence of the complete solid solution between hydroxy- and fluorapophyllites (Dunn *et al.*, 1978).

Another occurrence of apophyllite-type crystals, in a druse of albitite in a serpentine mass in the Kōmori Mine, Kyōto, has been described by Kurokawa (1967), but no chemical data were given. Three types of crystals were recognized optically, one of which was biaxial positive. The biaxial nature of the material and its association with albite suggest that it is probably similar to natroapophyllite or orthorhombic fluorapophyllite.

II. Crystal Structure

YASUNORI MIURA[2]

Department of Geology, University of Toronto
Toronto, Ontario M5S 1A1, Canada

TOSHIO KATO

Institute of Earth Sciences
Yamaguchi University, Yamaguchi 753, Japan

JOHN RUCKLIDGE

Department of Geology, University of Toronto
Toronto, Ontario M5S 1A1, Canada

AND HIROHARU MATSUEDA

Institute of Mining Geology
Akita University, Akita 010, Japan

Introduction

The chemical and crystallographic data presented in Part I suggest that fluorapophyllite and natroapophyllite are isostructural. Crystal structures of tetragonal potassium-rich fluorapophyllite have been determined by Taylor and Náray-Szabó (1931), and refined by Colville *et al.* (1971), Chao (1971), Prince (1971), and Bartl and Pfeifer (1976); and that of tetragonal potassium-rich hydroxyapophyllite by Rouse *et al.* (1978). Crystal structures of orthorhombic potassium-rich apophyllite (Sahama, 1965; Belsare, 1969), however, have not been determined because they are complexly twinned. It is well known that minor amounts of Na replace K in apophyllite, but no reports on the crystal structure of natural natroapophyllite with Na/K $\gg$ 1 have been published.

In this section the results of a crystal structure analysis of natroapophyllite (SA-1b) are given. The differential thermal analysis (DTA), thermogravimetric analysis (TGA) and IR absorption spectrum of the new mineral are also reported. Comparisons are made with tetragonal apophyllites of other workers. According to the redefinitions of Dunn *et al.* (1978) we refer to the latter as 'fluorapophyllite.'

[2] On leave from Department of Mineralogical Sciences and Geology, Faculty of Science, Yamaguchi University, Yamaguchi 753, Japan.

Experimental methods and results

A crystal 0.2 × 0.3 × 0.3 mm was mounted on a Syntex $P\bar{1}$ automated single-crystal diffractometer equipped with a graphite monochromator, at Kyūshū University. Mo$K\alpha$ radiation was used to measure 984 crystallographically-independent reflections up to $2\theta = 60°$, of which 563 reflections were judged to be significant ($I \geqq 3\sigma_I$). No absorption corrections were made, since the size and nature of the crystal was small enough for the effect to be negligible. The unit cell parameters $a = 8.875(4)$, $b = 8.881(6)$, $c = 15.79(1)$Å, $V = 1263.9$Å^3 were refined from the data for the 15 strong reflections used to orient the crystal on the Syntex $P\bar{1}$.

The crystal was from the Sampo Mine and was designated SA-1b. This was the most Na-rich among the specimens found there (Tables 1 and 2). Ten other specimens listed in Table 1 contain less Na, and are intermediate in composition between fluorapophyllite and natroapophyllite. The specimen which gave the sharpest reflections on Weissenberg photographs was SA-2, which originated in a druse in the white skarn. SA-1 and SA-3 specimens, on the other hand, yielded slightly diffuse spots, but showed more Na enrichment than SA-2. Figure 1(a) shows an optical micrograph of SA-1, where zoning due to Na–K substitution can be seen. The crystal (SA-1b) from SA-1 used for the structure determination was selected because it had the smallest cell parameters of

the six measured, and hence the highest Na content. Although it appeared to be optically homogeneous when placed in an oil cell in the spindle stage of a polarizing microscope, we cannot exclude the possibility that submicroscopic K-rich regions exist, and these might account for the diffuseness of the reflections. The composition assumed for this crystal (SA-1b) was that of the most Na-rich analysis found in SA-1 (see SA-1b in Table 2).

Starting parameters of the ions and water molecules in natroapophyllite were taken from the refinements of the fluorapophyllite structure by Colville *et al.* (1971) and Chao (1971). Their parameters were modified appropriately to account for Na substituting for K and the reduced symmetry (orthorhombic *vs.* tetragonal), which for most atoms causes a doubling of the number of independent atomic positions in an asymmetric unit. Hence Si(1) and Si(2) were derived from Si, O(2) and O(21) from O(2) and so on. Atom O(1), however, does not split. The O(1) site in the tetragonal cell lies on a two-fold axis at $z = \frac{1}{4}$ and has a multiplicity of 8. In the orthorhombic cell this site becomes a general position, again with a multiplicity of 8, but z is no longer constrained to the value $\frac{1}{4}$.

The refinement was carried out with the full-matrix least-squares program FLS4 written by Sakurai (1967).[3] Neutral atom scattering factors for Na, Ca, Si, F, and O were taken from the *International Tables for X-ray Crystallography Vol. IV* (1974); the 0.33 weight percent K indicated by the electron microprobe analysis (Table 1) was neglected. The reciprocal variances, $1/\sigma^2$, of the structure-factor amplitudes were used as weights in the refinement, except for unobserved reflections which were assigned zero weight. A three-dimensional difference Fourier synthesis was made and the possible positions of hydrogen atoms H(1), H(11), H(2), and H(21) were found in the map. However, the isotropic temperature factor of hydrogen atom H(21) was rather large (about 3), and hence this position is less well determined than the others.

The assignment of the space group of natroapophyllite to *Pnnm* was based on the results of running the data through the center of symmetry detection program RSWS3 written by Sakurai (1967). The presence of a center of symmetry is also supported by the fact that refinement converged in space group *Pnnm* to give an unweighted final residual of 0.056 compared with 0.3 when space group *Pnn*2 was tried. The final atomic parameters with their standard deviations are given in Table 4. The calculated interatomic distances and angles with errors are listed in Table 5.

Table 4. Atomic coordinates and isotropic temperature factors of natroapophyllite (SA-1b)

Atom	x	y	z	B
Si(1)	0.2289(3)*	0.0833(3)	0.1890(3)	1.12 (6)
Si(2)	0.4161(3)	0.2708(3)	0.3108(3)	1.13 (5)
Ca(1)	0.1143(3)	0.2465(3)	0	1.20 (6)
Ca(2)	0.7537(3)	0.1148(3)	0	1.25 (6)
Na	0	0	$\frac{1}{2}$	2.84(20)
F	0	0	0	1.87(24)
O(1)	0.3671(7)	0.1322(8)	0.2513(6)	1.36(13)
O(2)	0.0882(7)	0.1902(8)	0.2162(6)	1.63(15)
O(21)	0.3099(8)	0.4123(8)	0.2839(5)	1.59(14)
O(3)	0.2696(8)	0.0987(8)	0.0921(6)	1.75(15)
O(31)	0.4016(8)	0.2305(8)	0.4079(6)	1.66(14)
O(4)	0.2286(9)	0.4505(9)	0.0887(6)	2.45(18)
O(41)	0.5502(9)	0.2253(11)	0.0890(7)	2.70(19)
H(1)	0.47(1)	0.17(1)	0.05(1)	1.6
H(11)	0.17(1)	0.54(1)	0.08(1)	1.4
H(2)	0.16(1)	0.43(1)	0.14(1)	0.8
H(21)	0.56(2)	0.31(2)	0.14(1)	3.2

* *E.s.d.'s in parentheses refer to last digit.*

Natroapophyllite is built of sheets of four-membered rings of alternating tetrahedra (Fig. 3) with interleaving sheets containing the Ca and Na atoms. Natroapophyllite is essentially isostructural with apophyllite (Taylor and Náray-Szabó, 1931) and hydroxyapophyllite (Rouse *et al.*, 1978), with Na substituted for K and the ion pairs Si, Ca, O(2), O(3), O(4) having two independent sets of coordinates (Table 4) because of the lowering of symmetry from tetragonal to orthorhombic.

Si–O tetrahedra

The tetrahedra formed around the two Si atoms have slightly different configurations. The Si(1) ions are coordinated to O(1), O(2), O(21), and O(3). The Si(2) ions are coordinated to O(1), O(2), O(21) and O(31) (Figs. 4 and 5).

Figure 6 shows the Si(1)- and Si(2)-tetrahedra forming rings of four Si tetrahedra around the two-fold axis. Eight-membered rings of tetrahedra are also located in this plane, thus forming a layered structure parallel to the perfect {001} cleavage (Fig.

[3] To obtain a copy of a list of the observed and calculated structure-factor amplitudes, order document AM-81-154 from the Business Office, Mineralogical Society of America, 2000 Florida Ave., N.W., Washington, D.C. 20009. Please remit $1.00 in advance for the microfiche.

Table 5. Bond lengths and bond angles in natroapophyllite (SA-1b)

Bond lengths (Å)

SiO_4 Tetrahedra		Tetrahedra (O-O)		$Ca(O,F)_7$ Polyhedra	
Si(1)-O(1)	1.631(8)	O(1) -O(2)	2.589(9)	Ca(1)-O(3)	2.396(8)
-O(2)	1.626(7)	-O(21)	2.568(10)	-O(31)	2.392(8)
-O(21)	1.616(7)	-O(3)	2.675(12)	-O(4)	2.491(9)
-O(3)	1.578(10)	O(2) -O(21)	2.629(10)	mean	2.426
mean	1.613	-O(3)	2.662(11)		
		O(21)-O(3)	2.660(11)	Ca(2)-O(3)	2.399(11)
Si(2)-O(1)	1.608(8)	mean	2.631	-O(31)	2.213(8)
-O(2)	1.624(7)			-O(41)	2.490(10)
-O(21)	1.627(7)	O(1) -O(2)	2.569(10)	mean	2.367
-O(31)	1.579(9)	-O(21)	2.590(10)		
mean	1.610	-O(31)	2.640(12)	Ca(1)-F	2.413(3)
		O(2) -O(21)	2.632(10)	Ca(2)-F	2.412(3)
Si-Si		-O(31)	2.660(11)		
		O(21)-O(31)	2.665(11)	H_2O Molecules	
Si(1) -Si(2)	3.038(5)	mean	2.626		
Si(1)*-Si(2)	3.064(4)			H(1) -O(3)	2.0(1)
				-O(41)	1.1(1)
NaO_8 Polyhedron				H(11)-O(31)	1.8(1)
				-O(4)	1.0(1)
Na-O(4)	2.763(9)			H(2) -O(21)	2.6(1)
-O(41)	2.854(10)			-O(4)	1.0(1)
O(4)-O(41)	3.487(12)			H(21)-O(2)	2.3(1)
				-O(41)	1.1(1)

Bond Angles (degrees)

Tetrahedra (O-Si-O)				Tetrahedra (Si-O-Si)
O(1) -Si(1)-O(2)	105.3(4)	O(11)-Si(2)-O(2)	105.3(4)	Si(1)-O(1)-Si(1)
-O(21)	104.5(4)	-O(21)	106.4(4)	139.4(5)
-O(3)	112.9(4)	-O(31)	111.8(4)	Si(1)-O(2)-Si(2)
O(2) -Si(1)-O(21)	108.4(4)	O(2) -Si(2)-O(21)	108.2(4)	141.6(6)
-O(3)	112.4(4)	-O(31)	112.3(4)	Si(1)-O(21)-Si(2)
O(21)-Si(1)-O(3)	112.8(4)	O(21)-Si(2)-O(31)	112.4(4)	141.3(6)

* *The symmetry transform is given as follows:* $\frac{1}{2}+x$, $\frac{1}{2}-y$, $\frac{1}{2}-z$.

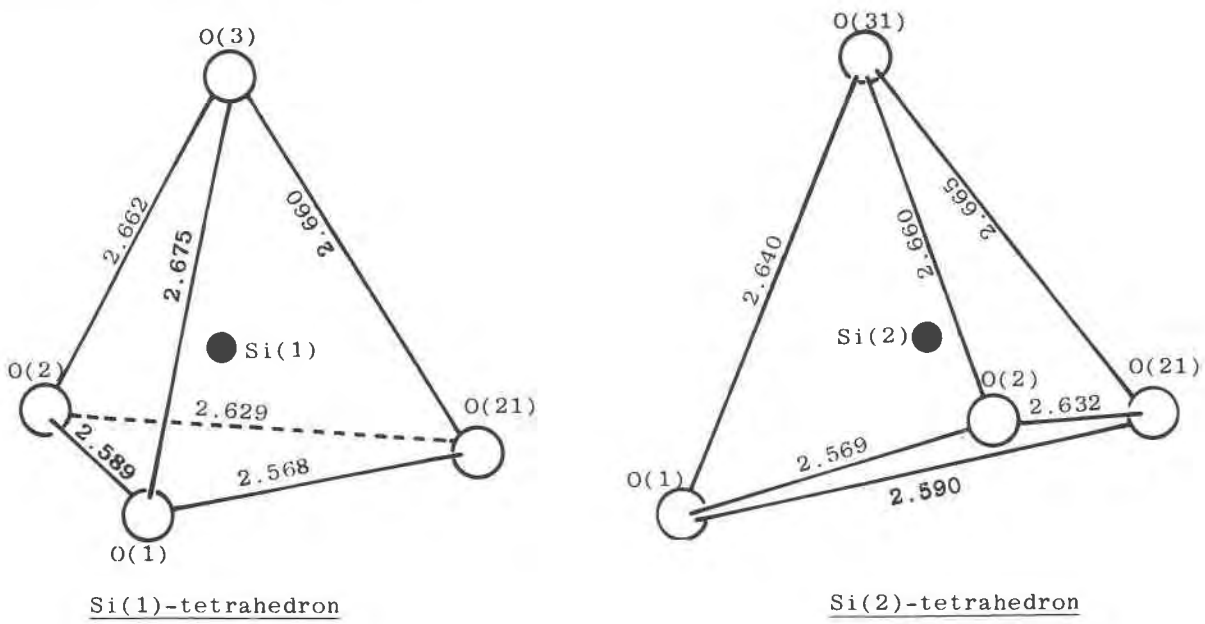

Fig. 4. Geometry of O–O distances of Si(1)- and Si(2)-tetrahedra in natroapophyllite.

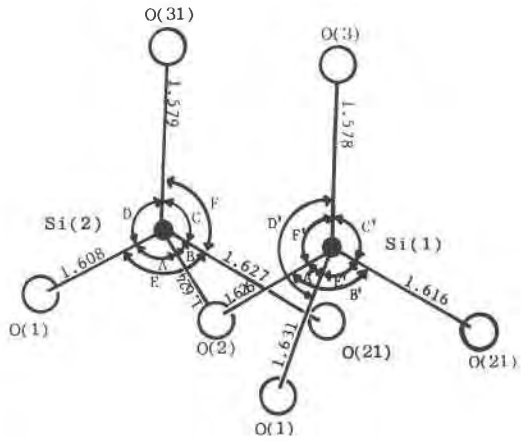

A=105.3	A'=105.3
B=108.2	B'=108.4
C=112.4	C'=112.8
D=111.8	D'=**112.9**
E=**106.4**	E'=104.5
F=112.3	F'=112.4

Fig. 5. Bond lengths in Å and bond angles in degrees of the Si(1)- and Si(2)-tetrahedra projected on (010).

3). Note the similarity of the apophyllite structure in this projection to that of sanidine when projected on the $(20\bar{1})$ plane (Ribbe, 1975). However, in apophyllite each of the tetrahedra in a four-membered ring points the same way, while in sanidine the two pairs comprising the ring point up and down, respectively.

In the tetrahedral layer, O(1) is shared between the Si(1)- and the Si(2)-tetrahedra which point upward and downward along the *c* axis. On the other hand, O(2) and O(21) are shared between Si(1)- and Si(2)-tetrahedra, which surround the Na atom and point in the same direction. Only the unshared oxygens, O(3) and O(31), are bonded to the interlayer Ca(1) and Ca(2) atoms (Figs. 6 and 7).

The Si(1)-tetrahedra have bond lengths which are longer to O(1) and shorter to O(3) and O(21) than those of fluorapophyllite. The mean distances of Si(1)-tetrahedra of natroapophyllite, however, are similar to those of tetragonal apophyllites (Table 6).

On the other hand, the Si(2) tetrahedra are distorted on account of O(1), O(31), and O(2), which are shifted significantly when compared with the oxygens of the Si(1) tetrahedra. The mean Si–O distance in the Si(2) tetrahedra is 1.610Å, which corresponds to the minimum value of the grand mean Si–O bond length in silicate structures (Brown and Gibbs, 1969). Figure 5 and Table 5 show that mean bond angles O–Si–O are similar to those of fluorapophyllite, both in the Si(1) and the Si(2) tetrahedra, but the bond angles O(1)–Si(2)–O(21) and O(1)–Si(2)–O(31) differ significantly from those of fluorapophyllite. The Si(1)–O(2)–Si(2) bond angles, 141.1° and 141.3°, are slightly larger than those of fluorapophyllite, 140.8° (Colville *et al.*, 1971; Chao, 1971; Bartl and Pfeifer, 1976).

Figure 3 shows the Si_8O_{20} sheet of natroapophyllite (SA-1b) projected on (001). The Si–O tetrahedra are slightly deformed by the shift of the atomic positions of O(1) and O(21), which have such a large effect on the distorted ring of four Si–O tetrahedra orthorhomic symmetry results. The displacement which largely affects the change of symmetry from tetrag-

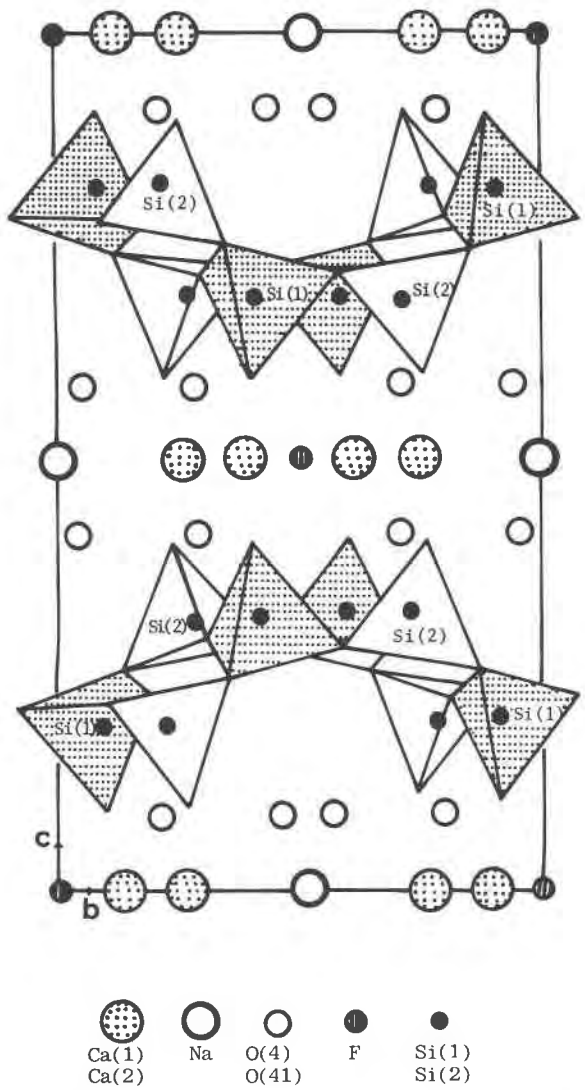

Fig. 6. The structure of natroapophyllite projected on (100).

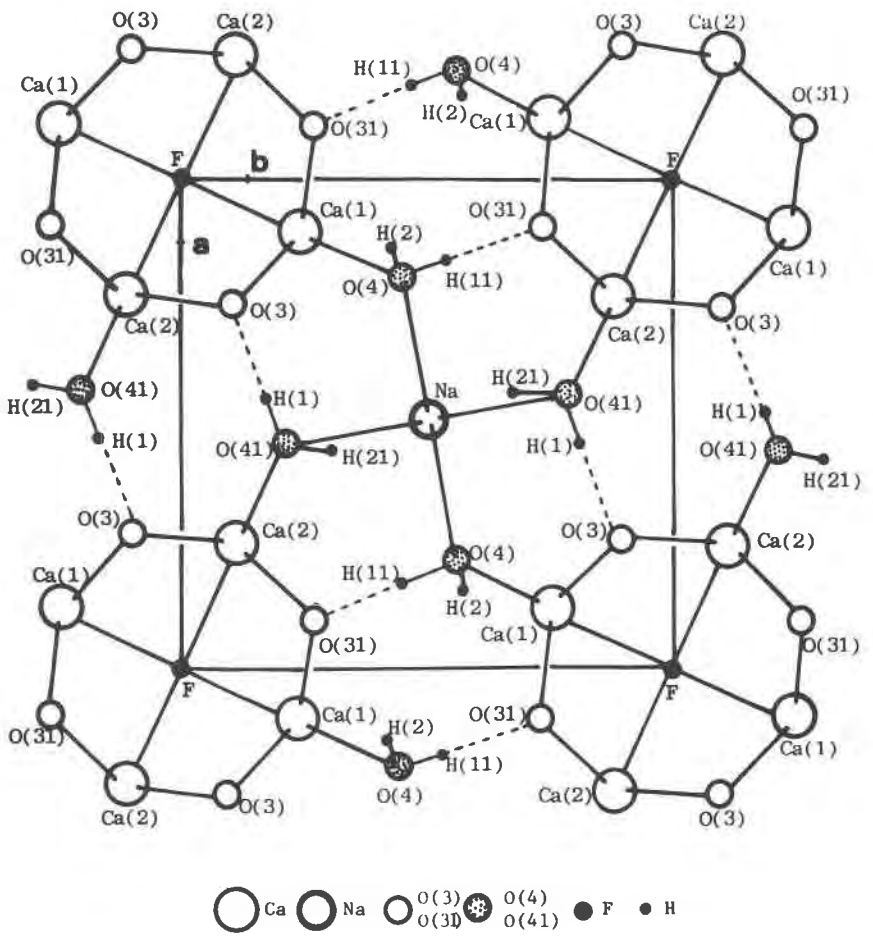

Fig. 7. The Na, and Ca(1) and Ca(2) sheet in natroapophyllite projected on (001). The probable positions of hydrogen atoms H(1), H(11), H(2), and H(21) are also shown.

onal to orthorhombic is not so marked in the Si tetrahedra as it is in the Na–O(4) bond lengths and O(41) positions as discussed below.

Ca–O polyhedra

Figure 7 shows the Na and Ca sheets in natroapophyllite projected on (001). The Ca(1) and Ca(2) atoms are bonded to O(4) and O(41), respectively, of the water molecules. These oxygens are shared with the Na atoms. The Ca(1) and Ca(2) are also bonded to four oxygens O(3) and O(31), and to the F atom. The mean Ca–O distance is similar to that in fluorapophyllite (Tables 5 and 6), but Ca(2)–O is significantly shorter, especially for Ca(2)–O(31). The distance of O(3) or O(31) between the upper and lower Si–O tetrahedra is 2.909Å, which is slightly shorter than in fluorapophyllite, 2.911 to 2.919Å (Colville *et al.*, 1971; Chao, 1971; Prince, 1971).

Na–O polyhedra

The Na atoms, whose ionic radii are less than those of K, replace the K atoms of apophyllite. In fact, the Na–O(4) or Na–O(41) bond lengths, 2.763 or 2.825Å, respectively, are shorter by about 5 percent on average than those of fluorapophyllite, as listed in Table 6. The smaller cell dimensions of natroapophyllite (SA-1b) are thus mainly due to the substitution of Na for K. This substitution also results in lowering the symmetry from tetragonal to orthorhombic.

H_2O molecules

In the final difference Fourier map, rather diffuse peaks were evident, which were taken to indicate the possible presence of the hydrogen atoms H(1), H(11), H(2), and H(21); but the atoms H(3) and H(31), cor-

Table 6. Selected mean interatomic distances (Å) of natroapophyllite (SA-1b) compared with those in the apophyllites previously reported

	Natroapophyllite (SA-3)		Colville *et al.* (1971)	Chao (1971)	Prince (1971)	Bartl and Pfeifer (1976)	Rouse *et al.* (1978)
Si - O	1.613	1.610	1.616	1.614	1.615	1.616	1.616
Ca - O	2.426	2.367	2.427	2.422	2.430	2.422	2.435
Ca - F,OH	2.413	2.412	2.416	2.418	2.429	2.414	2.435
Na,K - O	2.763	2.854	2.972	2.971	2.950	2.965	2.954
O(4) - O(41)	3.487		3.690	3.694	---	---	3.672
Tetrahedra (O - O)	2.631	2.626	2.636	2.632	---	---	2.637
H(1) - O(3)	2.0	1.8	---	1.827	1.762	1.772	} 2.743
- O(4)	1.0	1.1	---	0.968	0.983	0.983	
H(2) - O(2)	2.3	2.6	---	2.693	2.269	2.260	} 3.312
- O(4)	1.0	1.1	---	0.552	0.958	0.953	

responding to the H(3) reported by Prince (1971) and Bartl and Pfeifer (1976), could not be found in the expected positions. Tables 5 and 6 show that the H–O bond lengths are similar to those of fluorapophyllite. But the relaxation allowed by the orthorhombic symmetry results in slight changes in the geometry O(3)–H(1)–O(41)–H(21)–O(2) and O(31)–H(11)–O(4)–H(21) configurations, which would be identical in the case of tetragonal symmetry. The angles H(1)–O(41)–H(21) and H(11)–O(4)–H(2) are 111(7)° and 94(9)°, respectively; the angles O(2)–H(21)–O(41) and O(21)–H(2)–O(4) are 137(11)° and 176(9)°; and the angles O(3)–H(1)–O(41) and O(31)–H(11)–O(4) are 124(9)° and 157(11)°. That these differences may be significant is supported by the independent DTA and IR data discussed below.

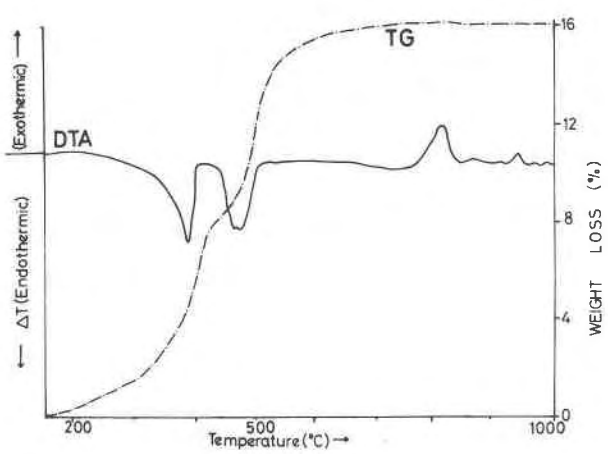

Fig. 8. Differential thermal and gravimetric analysis curves for natroapophyllite (SA-1b) from the Sampo Mine.

DTA and TGA curves

Differential thermal analysis of natroapophyllite (Fig. 8), heated in air at the rate of 12°C/min, shows two main endothermic peaks at 380° and 460°C. The peak at 460°C is broader, with two barely distinguishable maxima at 455° and 468°C (Table 7). With the exception of the doubling of the second peak, the curve is similar to those reported for fluorapophyllite by Colville *et al.* (1971), Chao (1971), and Bartl and Pfeifer (1976). The same interpretation given for apophyllite is applicable to the DTA curve for this specimen; namely, the first and second broad peaks occurring at the different stages may be due to loss of H_2O and HF, respectively. The latter molecule may be formed at higher temperature, as pointed out by Colville *et al.* (1971), Chao (1971), Prince (1971) and Bartl and Pfeifer (1976).

Thermal gravimetric analysis, run in air at a heating rate of 6°C/min, shows that water loss starts at about 160°C and continues until a discontinuity between 410° and 500°C, as shown in Figure 8. The dehydration is more rapid until it reaches 16 percent total weight loss at 700°C, which is similar to that of fluorapophyllite (Colville *et al.*, 1971; Chao, 1971; Bartl and Pfeifer, 1976).

IR spectrum

Figure 9 shows the OH stretching vibration and absorbed water regions of the IR spectrum of natroapophyllite (SA-1b). The spectrum shows two sharp absorption bands at 3560 and 3420 cm^{-1}, and a broad band at about 3020 cm^{-1}.

Table 7. Endothermic peaks, dehydration and IR absorption bands of natroapophyllite (SA-1b) and the apophyllites previously reported

Specimens	Endothermic peaks (°C) (DTA data)	Dehydration (°C) (TGA data)	Absorption bands (in cm^{-1}) (IR data)
Kamioka apophyllite (Koizumi, 1953)	334 440	280 280~440	---
Phoenix apophyllite (Colville *et al.*, 1971)	325 450	225~600	3560(sharp) 3070(broad)
Mont. St. Hilaire apophyllite (Chao, 1971)	350 375 468	250	---
Centerville apophyllite (Prince, 1971)	325	---	---
Apophyllite (Bartl and Pfeifer, 1976)	320 350 450	200~320 320~580	---
Sampo natroapophyllite (in this study)	380 455 468	160~500	3560(sharp) 3420(sharp) 3020(broad)

Discussion

An extension of the interpretation given by Colville *et al.* (1971) for fluorapophyllite can be applied to the IR data. They concluded that their sharp absorption band at 3560 cm^{-1} indicated a weak hydrogen bond, while their broad band at 3070 cm^{-1} meant a stronger one. In our spectrum, two sharp absorption bands occur in the 3500 cm^{-1} region, which suggests that there are two weaker hydrogen bonds of slightly different strengths. Combining the results of the IR data and the crystal structure analysis leads to the conclusion that there are three (and possibly four) different structural environments for the hydrogen atoms in the water molecules. Table 5 shows that the bonds H(1)–O(3), H(11)–O(31), H(2)–O(21), and H(21)–O(2) are 2.0, 1.8, 2.6, and 2.3Å respectively.

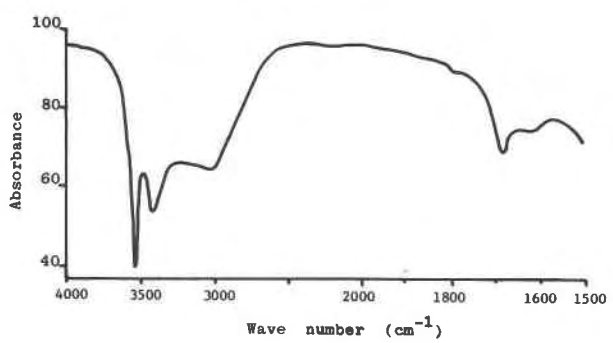

Fig. 9. IR absorption spectrum for natroapophyllite (SA-1b) from the Sampo Mine.

The latter two, being the longer, are therefore the weaker and account for the two sharp absorption bands at 3560 and 3420 cm^{-1}. the former two are shorter but give broad absorption bands which overlap and are not resolved in the spectrum.

The doubling of the sharp band in the 3500 cm^{-1} region is a direct consequence of the orthorhombic symmetry, and provides satisfying confirmation that the data from independent methods are consistent with each other. It also suggests a rapid method for testing for orthorhombic symmetry in the apophyllite group. As mentioned above, the DTA curve shows a broad endothermic peak with two maxima at 455° and 468°C. This doubling, which is not seen in any of the curves reported for tetragonal apophyllites, could conceivably also arise from the lowered symmetry. However, it would be unwise to place too much weight on these rather tenuous data.

The crystal structure of natroapophyllite is isostructural with that of fluorapophyllite, with allowance made for the reduction in symmetry from tetragonal to orthorhombic. In order to establish where the symmetry change takes place in the K–Na substitution series, and how much solid solution exists, systematic structure determinations and IR measurements of other samples with compositions intermediate between fluorapophyllite and natroapophyllite are required. In view of the diffuseness of the reflections from the most Na-rich crystals, high-resolution transmission electron microscopy may be informative.

Acknowledgments

We thank Dr. A. Kato of the National Science Museum, Japan for valuable suggestions regarding the naming of this new mineral; Dr. J. S. White, National Museum of Natural History, Smithsonian Institution, Washington, D.C. for valuable discussions; Dr. T. Watenabe of Kyūshū University for his help in the DTA, TGA and IR measurements.

The calculations were carried out on the FACOM M-200 at the Computer Center of Kyūshū University and also on the HITAC 8800 computer at Tōkyo University. Y. Miura acknowledges a fellowship from the National Sciences and Engineering Research Council of Canada under which this work was completed.

Drs. R. C. Ewing and P. Dunn are thanked for their critical comments on the manuscript.

References

Appleman, D. E. and Evans, H. T. Jr. (1973) Job 9214: Indexing and least-squares refinement of powder diffraction data. U.S. Dept. of Commerce Technical Information Service, PB216, 188.

Bartl, H. and Pfeifer, G. (1976) Neutronenbeugungsanalyse des Apophyllit $KCa_4(Si_4O_{10})_2(F/OH) \cdot 8H_2O$. Neues Jahrbuch für Mineralogie Monatshefte, 58–65.

Belsare, M. R. (1969) A chemical study of apophyllite from Poona. Mineralogical Magazine, 37, 288–289.

Brown, G. E. and Gibbs, G. V. (1969) Oxygen coordination and the Si–O bond. American Mineralogist, 54, 1528–1539.

Chao, G. Y. (1971) The refinement of the crystal structure of apophyllite. II. Determination of the hydrogen positions by X-ray diffraction. American Mineralogist, 56, 1234–1242.

Colville, A. A., Anderson, C. P., and Black, P. M. (1971) Refinement of the crystal structure of apophyllite. I. X-ray diffraction and physical properties. American Mineralogist, 56, 1222–1233.

Dunn, P. J. and Wilson, W. E. (1978) Nomenclature revisions in the apophyllite group: hydroxyapophyllite, apophyllite, fluorapophyllite. Mineralogical Record, 3, 95–98.

Dunn, P. J., Rouse, R. C. and Norberg, J. A. (1978) Hydroxyapophyllite, a new mineral, and a redefinition of the apophyllite group. I. Description, occurrences and nomenclature. American Mineralogist, 63, 196–199.

Koizumi, M. (1953) The differential thermal analysis curves and the dehydration curves of zeolites. Mineralogical Journal, 1, 36–47.

Kurokawa, K. (1967) Apophyllite found in the Kōmori Ultrabasic Mass (in Japanese). Journal of Japanese Association of Mineralogists, Petrologists, and Economic Geologists, 57(6), 232–237.

Matsueda, H. (1973) On the mode of occurrence and mineral paragenesis of iron-wollastonite (ferro-bustamite) skarn in the Sampo Mine, Okayama Prefecture (in Japanese). Science Reports, Department of Geology, Kyūshū University, 11, 265–273.

Matsueda, H. (1975) "Na-apophyllite" from the skarn of the Sampo Mine, Okayama Prefecture, Japan (abstract, in Japanese). Annual Joint Meeting of Japanese Association of Mineralogists, Petrologists, and Economic Geologists; Mineralogical Society of Japan; and Mining Geology. Abstracts with Program (Kōfu), 75.

Matsueda, H. (1980) Pyrometasomatic iron-copper ore deposits of the Sampo Mine, Okayama Prefecture. Part I. Geology and Mineralogy. Journal of Mining College, Akita University, Series A, 5(4), 15–77.

Miura, Y. (1977) Cation distribution and physical properties in apophyllite-type structure (abstract, in Japanese). Annual Meeting of Japanese Crystallographic Society. Abstracts with Program, 1B-3.

Miura, Y. and J. C. Rucklidge (1979) Variations in apophyllite structure and chemistry (abstract). American Crystallographic Association. Abstracts with Program (Honolulu), Series 2, 6(2), 89.

Miura, Y., Matsueda, H. and T. Kato (1976) Crystal structure of Na-substituted apophyllite from the Sampo Mine, Okayama (abstract, in Japanese). Annual Meeting of Mineralogical Society of Japan. Abstracts with Program, 130.

Prince, E. (1971) Refinement of the crystal structure of apophyllite. III. Determination of the hydrogen positions by neutron diffraction. American Mineralogist, 56, 1243–1251.

Ribbe, P. H. (1975) The chemistry, structure, and nomenclature of feldspars. In P. H. Ribbe, Ed., Feldspar Mineralogy. Mineralogical Society of America, Short Course Notes 2, R1-R52.

Rouse, R. C., Peacor, D. R. and Dunn, P. J. (1978) Hydroxyapophyllite, a new mineral, and a redefinition of the apophyllite group. II. Crystal structure. American Mineralogist, 63, 199–202.

Sahama, Th. G. (1965) Yellow apophyllite from Korsnas, Finland. Mineralogical Magazine, 34, 406–415.

Sakurai, T. (1965) Universal Crystallographic Computation Program System. Crystallogr. Soc. Japan, Tokyo.

Taylor, W. H. and Náray-Szabó, St. (1931) The structure of apophyllite. Zeitschrift für Kristallographie, 77, 146–158.

Manuscript received, October 15, 1979;
accepted for publication, October 30, 1980.